Author/s:
Gómez, DE;Shi, X;Oshikiri, T;Roberts, A;Misawa, H

Title:
Near-Perfect Absorption of Light by Coherent Plasmon-Exciton States

Date:
2021-05-12

Citation:
Gómez, D. E., Shi, X., Oshikiri, T., Roberts, A. & Misawa, H. (2021). Near-Perfect Absorption of Light by Coherent Plasmon-Exciton States. Nano Letters, 21 (9), pp.3864-3870. https://doi.org/10.1021/acs.nanolett.1c00389.

Near–perfect absorption of light by coherent plasmon-exciton states

Daniel E. Gómez,[*,†] Xu Shi,[‡] Tomoya Oshikiri,[‡] Ann Roberts,[¶] and Hiroaki Misawa[*,‡,§]

†*School of Science, RMIT University, Melbourne, VIC, 3000, Australia.*

‡*Research Institute for Electronic Science, Hokkaido University, Sapporo 001-0021, Japan*

¶*School of Physics, The University of Melbourne, VIC 3010, Australia*

§*Center for Emergent Functional Matter Science, National Chiao Tung University 30010, Taiwan*

E-mail: daniel.gomez@rmit.edu.au; misawa@es.hokudai.ac.jp

Abstract

We experimentally demonstrate and theoretically study the formation of coherent plasmon–exciton states which exhibit absorption of $> 90\%$ of the incident light (at resonance) and cancellation of absorption. These coherent states result from the interaction between a material supporting an electronic excitation and a plasmonic structure capable of (near) perfect absorption of light. We illustrate the potential implications of these coherent states by measuring the charge separation attainable after photo–excitation. Our study opens the prospect for realizing devices that exploit coherent effects in applications.

Keywords

Plasmonics, hot–charge carriers, ultra–fast spectroscopy, strong coupling

Coherent phenomena that arise from light–matter interactions result in unexpected modification of material properties. In the strong light–matter interaction limit, the excited states of a material proximate to an optical cavity are *polariton states*: hybrid light–matter states which possess properties that are different to those of the cavity and material alone.[1,2] The changes in the excited-state energetics that arise from strong coupling have led to a number of unexpected observations, including new (ultra–fast) energy relaxation pathways,[3,4] modified chemical reactivity,[5,6] enhanced photo–induced electron transfer[7,8] and changes to the work function of materials;[9] properties that were originally thought to be intrinsic to material composition alone. The coherent and spatially delocalized nature of polariton states can result in both augmented electrical conductivity,[10] and in–phase light emission[11] from molecules separated by as much as a hundreds of nanometres.[12] Remarkably, the coherent nature of these interactions enable efficient energy transfer across distances that are beyond those possible *via* standard mechanisms,[13,14] raising the prospect of exploiting coherent light-matter interactions to produce new mechanisms for harnessing light energy in efficient and unconventional ways.

Efficient absorption of light is an important operational aspect for any scheme that aims to harness radiant energy. Hybrid light–matter states result when there is reversible exchange of energy between light and material excitations at a rate that is at least comparable to the ones responsible for other dissipative processes. Consequently, it is counter intuitive to think that it would be possible to engineer systems that simultaneously enable the existence of light–matter coherent states and the conditions of critical coupling required for achieving high (or perfect) absorption of light. Critical coupling can occur when the radiative rate of a system is modified so that it matches the rate of its total absorptive losses. This condition of increased radiative rates therefore seems at odds with the seemingly closed nature of the reversible exchange of energy needed for realising hybrid light–matter states. However, near–perfect energy feeding into these kinds of states has been achieved *via* interferometric control of absorption using multiple beams of light, an approach that imposes stringent conditions

on the relative phase of the light beams, limiting the potential deployment of this concept into multiple areas of application.[15,16]

Here we show that near–perfect energy absorption by coherent light–matter states can be realised without such complex interferometric control in a scalable system comprised of a monolayer of gold nanoparticles in direct contact with molecular excitons, both interacting with incident light and an optical resonance supported by a Fabry–Pérot (FP) cavity (Figure 1a). The cavity modifies the radiative rate of the metal nanoparticles, leading to a condition of (near) critical coupling, which is manifest by an absorption of $> 90\%$ of the incident light at the resonant frequencies.

Coupled Mode Theory. As a starting point, we theoretically investigate the interactions among light, a localized surface plasmon resonance and excitons. Although in principle one should use quantum mechanics of open systems,[17,18] physical insight can be obtained through a coupled–mode theory,[19,20] from which it is possible to determine the reflection coefficient of the system, enabling a direct comparison to measured spectra. To this end, we consider a system of two oscillators (each characterised by a resonance frequency ω_p and ω_x) that interact with incident light *via* a single channel and, furthermore, we assume that no transmission of light is possible (due to a mirror, Figure 1a). p and x are the amplitude of oscillations in each, noting that these are normalised so that $|p|^2$ and $|x|^2$ correspond to the energy contained in each oscillator. Both oscillators reversibly exchange energy with each other at a rate given by Ω, and with the incident light (which carries an amount of power $|s_+|^2$) *via* radiative rates $\gamma^{\mathrm{r}}_{p,x}$. Additionally, we consider non–radiative energy dissipation with the rates $\gamma^{\mathrm{nr}}_{p,x}$. Conservation of energy[20,21] requires an additional interaction mechanism between both oscillators, accounted for by a rate $\gamma_o = \sqrt{\gamma^{\mathrm{r}}_p \, \gamma^{\mathrm{r}}_x}$, which resembles the Agarwal-Fano coupling terms that explains virtual emission and reabsorption of radiation between the p and x.[22] With all of these considerations in mind, the time–evolution of the

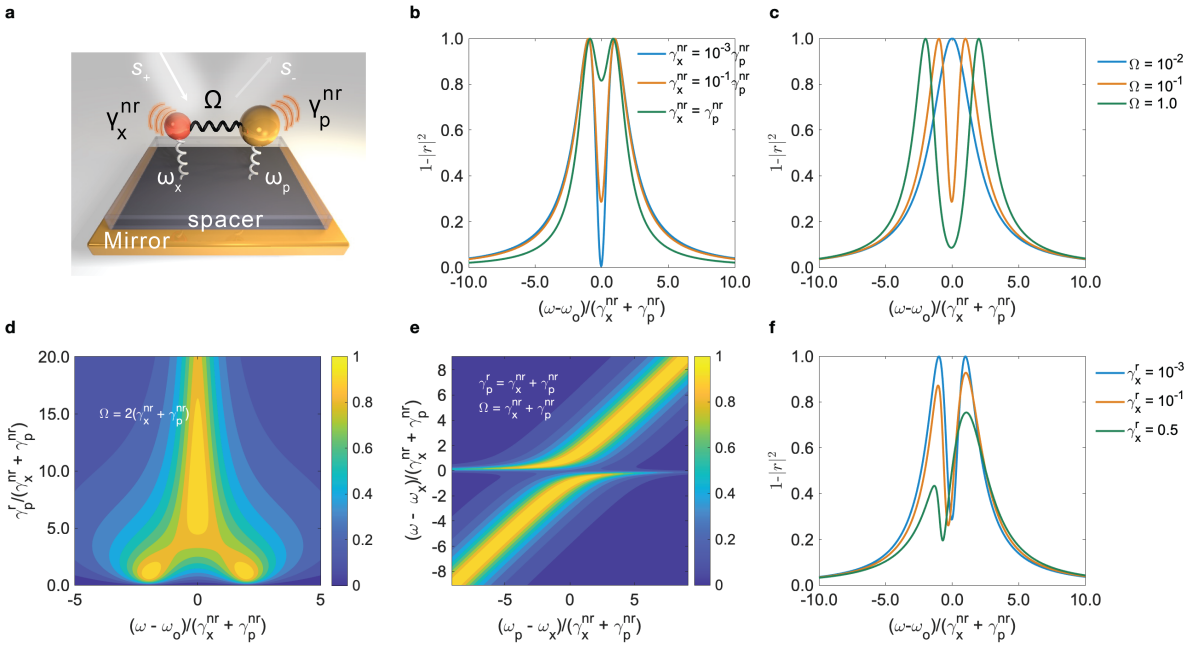

Figure 1: **Perfect absorption of light and coherent interactions** (**a**) Schematic representation of the interacting plasmon–exciton system described by equation (1). Incident light (carrying $|s_+|^2$ power) interacts with two types of oscillators (each characterised by a resonance frequency $\omega_{p,x}$). Both sub–systems reversibly exchange energy with each other at a rate Ω, can radiate into outgoing waves s_-, and can also experience non–radiative losses described by the rates $\gamma^{\rm nr}_{p,x}$. (**b**) Effect of the non–radiative rate $\gamma^{\rm nr}_x$ on the cancellation of absorption. The system is assumed to be operating under critical coupling and $\Omega = (\gamma^{\rm nr}_p + \gamma^{\rm nr}_x)$. (**c**) Effect of Ω on the extent of cancellation of absorption (the values in the legend are multiples of $(\gamma^{\rm nr}_p + \gamma^{\rm nr}_x)$). The system is assumed to be operating under critical coupling. (**d**) As the radiative rate of the plasmon system is scanned, there is a coalescence of a doublet into a single band exhibiting perfect absorption (The case is shown for $\omega_p = \omega_x = \omega_o$). (**e**) The induced transparency persists even when the plasmon and exciton sub–systems are detuned $[\gamma^{\rm r}_x = 10^{-3}(\gamma^{\rm nr}_p + \gamma^{\rm nr}_x)]$. (**f**) Effect of the magnitude of $\gamma^{\rm r}_x$ on the absorption at the critical coupling condition. The values quoted in the legend are relative to $(\gamma^{\rm nr}_p + \gamma^{\rm nr}_x)$.

p and x system is written:

$$\begin{aligned}\frac{dp}{dt} &= (i\omega_p - \gamma_p^{\mathrm{r}} - \gamma_p^{\mathrm{nr}})p + (i\Omega - \gamma_o)x + \sqrt{2\gamma_p^{\mathrm{r}}}\, s_+, \\ \frac{dx}{dt} &= (i\omega_x - \gamma_x^{\mathrm{r}} - \gamma_x^{\mathrm{nr}})x + (i\Omega - \gamma_o)p + \sqrt{2\gamma_x^{\mathrm{r}}}\, s_+.\end{aligned} \tag{1}$$

The system of oscillators couple energy into the outgoing waves (s_-): $s_- = -s_+ + p\sqrt{2\gamma_p^{\mathrm{r}}} + x\sqrt{2\gamma_p^{\mathrm{r}}}$, which enables the definition of a complex reflection coefficient $r = s_-/s_+$, for which a closed analytical form can be obtained (see supporting information). With this theory, it is possible to make important predictions, including (i) the cancellation of absorption and (ii) the occurrence of perfect absorption, as we now discuss.

There is a frequency ω_t at which absorption vanishes (*i.e.* $r = 1$, Figure 1b) and it is given as a radiative–rate–weighted average of the resonant oscillation frequencies:

$$\omega_t = \frac{\gamma_p^r\omega_x + \gamma_x^r\omega_p - 2\Omega\sqrt{\gamma_x^r\gamma_p^r}}{\gamma_x^r + \gamma_p^r}.$$

In other words, in the absence of non–radiative losses, a coherent interaction between both oscillators, controlled by their radiative rates, results in the cancellation of absorption. This is a classical analogue of electromagnetically induced transparency,[23] which has been experimentally demonstrated with whispering gallery mode resonators,[24] metamaterials/metasurfaces,[25,26] plasmonic[27] and plasmon–exciton systems.[28] The extent of the cancellation of absorption decreases as the non–radiative rate of the exciton system increases (Figure 1b), and the spectral lineshape around this decreased absorption point depends on the value of the coupling strength Ω (Figure 1c). The effect can be seen to disappear for vanishingly small values of Ω (Figure 1c).

There are two set of circumstances under which the model results in closed analytical conditions for perfect absorption (*i.e.* $r = 0$). In the limit where both oscillators have identical resonance frequencies ($\omega_p = \omega_x$), and the radiative rate of one of the oscillators is vanishingly small (*i.e.* $\gamma_x^r \sim 0$, making it a "dark" oscillator), perfect absorption can occur

at a single spectral band centred at ω_o when the radiative rate $\gamma_p^{\mathrm{r}} = \Omega^2/\gamma_x^{\mathrm{nr}} + \gamma_p^{\mathrm{nr}}$. Secondly, it can also take place at two bands $\omega_\pm$ which are separated in energy by an amount:

$$\omega_+ - \omega_- = 2\sqrt{\Omega^2 - (\gamma_x^{\mathrm{nr}})^2}, \tag{2}$$

whenever the radiative rate matches the total non–radiative dissipation rate of the system:

$$\gamma_p^r = \gamma_p^{\mathrm{nr}} + \gamma_x^{\mathrm{nr}}, \tag{3}$$

corresponding to a critical coupling condition (details in the supporting information). In order to observe two distinct absorption bands, both oscillators need to exchange energy faster that the dissipation rate of the "darker" oscillator: $\Omega > \gamma_x^{\mathrm{nr}}$, and clearly, the condition on the radiative rate γ_p^{r} is independent to the one on the coupling constant Ω, indicating that it is possible to achieve perfect absorption into the coherently coupled states with resonant frequencies $\omega_\pm$.

Perfect absorption is illustrated in Figure 1d, where it can be observed that as the radiative rate γ_p^{r} increases, the system enters into critical coupling resulting in two spectral bands with perfect absorption (*i.e.* $1 - |r|^2 = 1$). As the rate γ_p^{r} is increased further, these two absorption bands coalesce into a single band, in a way that is akin to what is observed for systems exhibiting resonant exceptional points.[29]

Away from the resonance condition $\omega_p = \omega_x$, it is still possible to observe high values of absorption into spectral doublets (Figure 1e). As the resonant frequency of one of the sub–systems is scanned (*i.e.* ω_p relative to ω_x), the resulting energy dispersion curve exhibits an avoided crossing, which is normally associated with strong coupling.[1]

Near–perfect absorption of light (*i.e.* $r \sim 0$) can also be observed for the case where both oscillators are "bright" (*i.e.* $\gamma_x^{\mathrm{r}} \neq 0$, Figure 1f). In this case there is *asymmetric* absorption at $\omega_\pm$, and the extent of the asymmetry increases with γ_x^{r}.

Experimental realisation To realise the system described in Figure 1a, we employed

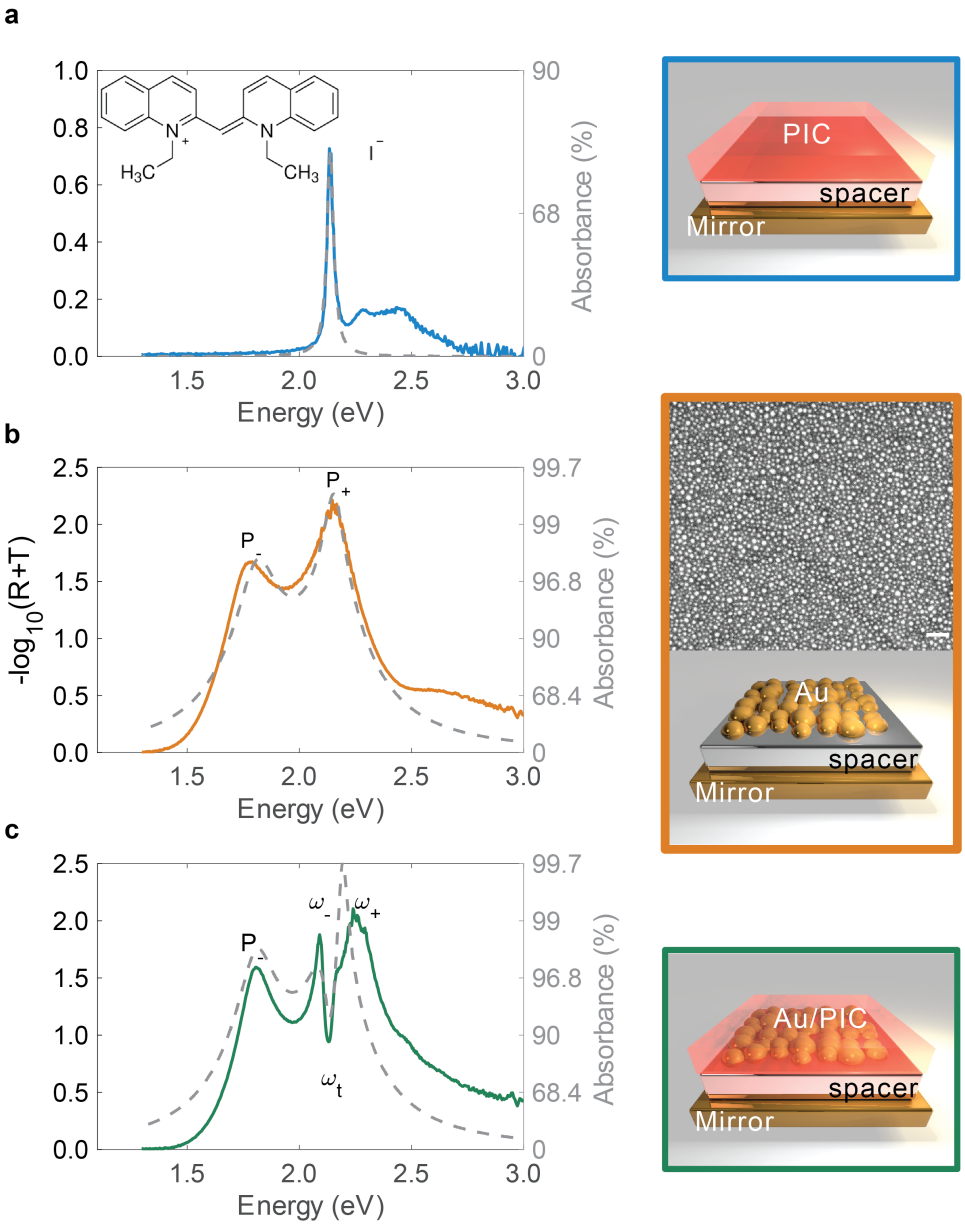

Figure 2: **Plasmon - exciton (near) perfect absorption of light**. **a** Absorption spectrum of a thin polymer film doped with PIC (structure shown as an inset) deposited on top of a Mirror/TiO_2 support. **b** Absorption spectrum of a Mirror/TiO_2/Au nanoparticle system (covered with a polymer film without PIC). The system exhibits strong plasmon-cavity coupling, as evidenced by the appearance of a spectral doublet. A representative SEM image is also shown, where the scale bar corresponds to 100 nm. **c** Absorption spectrum of a system of interacting plasmons and excitons both supported on a Mirror/TiO_2 film. There is a clear manifestation of the coherent effects described in Figure 1. In all cases, the dashed line is a fit to a model based on equation (1) as described in the text.

molecular J–aggregates of pseudo isocyanine (PIC, chemical structure shown in the Figure 2a) as the exciton material and a monolayer of gold nanoparticles as the plasmonic sub–system. Both of these are supported on a mirror–spacer thin film which ensures a single channel operation, as light can only effectively interact with the materials through one side of the sample, and furthermore, it enables the manipulation of the radiative rate of the metal nanoparticles.[30–32] The nanoparticle–spacer–mirror configuration, in particular, the thickness of the spacer layer, was previously optimized to ensure spectral overlap between one of

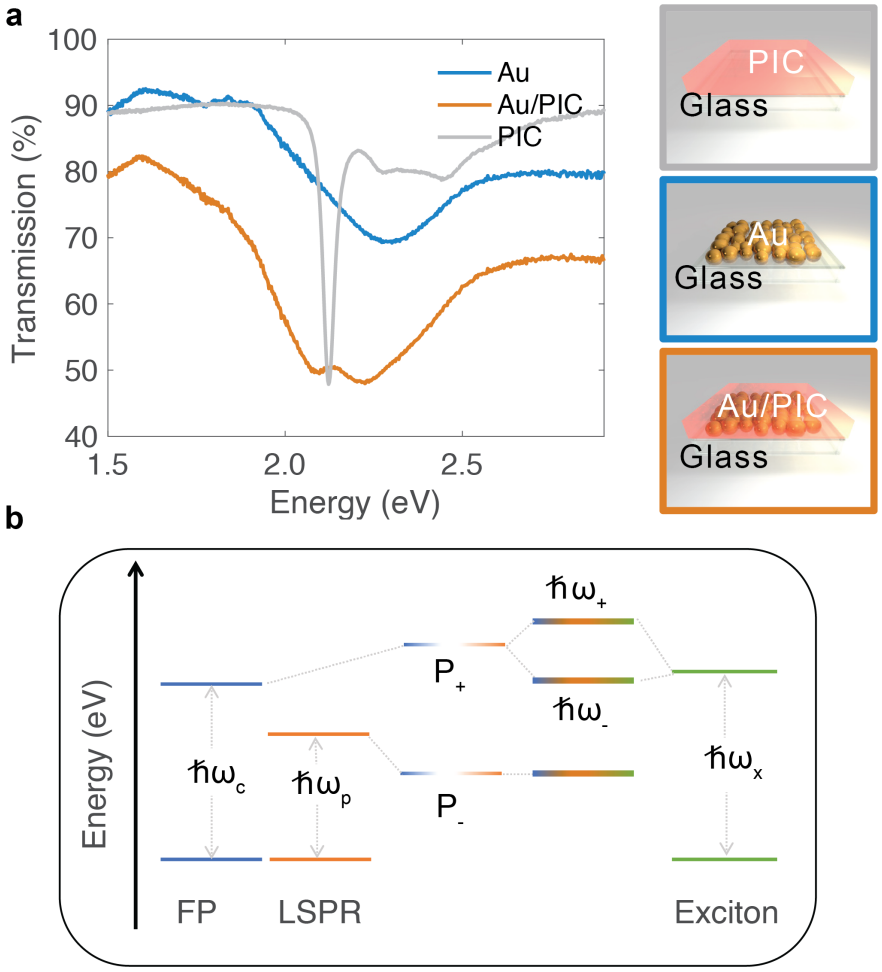

Figure 3: **Plasmon – exciton interactions**. **a** In the absence of (near) perfect absorption, a monolayer of Au particles (blue) exhibits a single spectral band due to the excitation of localised surface plasmon resonances. When both plasmon and excitons (PIC, grey line) interact, a moderate splitting occurs (orange). **b** Hybridisation diagram. The horizontal scale represents an energy scale. Three sub–systems are considered a Fabry–Pérot (FP), a localised surface plasmon resonance (LSPR) and and exciton resonance.

its optical resonances and the exciton absorption band of the molecular J–aggregates.[33]

The absorption spectrum of a thin polymer film doped with PIC, deposited on a Au mirror / TiO_2 film support, displays a sharp band at $\hbar\omega_x \sim 2.14$ eV (580 nm) (Figure 2a), which is due to Frenkel exciton states that originate due to molecular J aggregation.[34] The dashed line in Figure 2a is a fit to a coupled–mode–theory model for a single oscillator,[21] resulting in a value for $\hbar\gamma_x^{\mathrm{r}} = 7.6$ meV and $\hbar\gamma_x^{\mathrm{nr}} = 19.3$ meV.

In the absence of the mirror/TiO_2 support, the transmission spectrum of a monolayer of gold nanoparticles supported on a glass substrate and covered with a thin polymer film (SEM in Figure 2b) is characterised by a single band with a line width of ~ 179 meV, which is due to the excitation of localised surface plasmon resonances (LSPRs) in the population of nanoparticles. The mirror–spacer–nanoparticle layer system can exhibit hybrid excitations due to the interaction of localised surface plasmon and optical FP resonances (Figure 2b).[32,33,35] This is manifest in the optical absorption spectra by the appearance of spectral doublets (located at positions indicated with P_+ and P_- in Figure 2b), corresponding to the excitation of hybrid modes where the energy is strongly localised either as a cavity–like mode (P_-) or in the near–field of the metal nanoparticles (P_+).[36] Due to modifications in the radiative rate γ_p^{r} of the particle plasmon resonance, the system can exhibit high levels of optical absorption, in line with the discussion made in relation to Figure 1d. At frequencies close to the optical resonances, the spectra can be well–described using the coupled–mode–theory of equation (1) (with the oscillator x substituted for the FP resonant mode, denoted with a subscript c, and furthermore, assuming $\gamma_c^{\mathrm{r}} = 0$). The result of this analysis is shown in Figure 2b with a dashed line resulting in a value of the plasmon-cavity coupling of $\hbar\Omega = 236$ meV, a cavity non–radiative decay rate of $\hbar\gamma_c^{\mathrm{nr}} = 218$ meV (with a cavity quality factor $Q \sim 9$), and plasmon resonance rates $\hbar\gamma_p^{\mathrm{r}} = 289$ meV, $\hbar\gamma_p^{\mathrm{nr}} = 179$ meV which given that $\Omega > \gamma_c^{\mathrm{nr}}$, justifies why the spectrum exhibits two absorption bands. The values obtained for the radiative and non–radiative rates indicate that the plasmon–cavity system is close to the critical coupling condition of equation (3), which explains the high

level of absorption measured ($\gtrsim 99\%$, Figure 2b).

Figure 2c shows the results obtained for the mirror–spacer–nanoparticle–exciton system. When the J–aggregates are placed in the optical near–field of the metal nanoparticles, plasmon–exciton interactions lead to a moderate splitting of the measured optical transmission spectrum (orange line in Figure 3a).[1,28] The magnitude of the splitting, given by $\mu \cdot \mathbf{E}$ (where μ is the excited-state dipole moment of the exciton and $\mathbf{E}$ the electric field due to the particle plasmon resonance) is in this case comparable to the linewidth of the LSPR, which in turn is likely to be broadened due to the distribution of sizes and shapes obtained during the fabrication of the nanoparticle film.

The exciton transition is nearly resonant with the P_+ plasmon–cavity hybrid mode. When both particle plasmons and excitons interact in the presence of the mirror/TiO_2 support, the measured absorption spectrum consists of three bands (labelled P_-, ω_- and ω_+ in Figure 2c). The lowest–energy band occurs at almost the same energy as P_- of Figure 2b. Due to coherent plasmon–exciton interactions, the P_+ band and the exciton transition split into two absorption maxima $\omega_\pm$, with absorbances of $\sim 99\%$ and an opening of a window of reduced absorption (ω_t, Figure 2c). The magnitude of the splitting of the two bands depends on the concentration of J aggregates in the film, and the cancellation of absorption completely disappears for low concentrations of the J–aggregates (Figure S4). This is in line with the predictions made in Figure 1c, as the plasmon–exciton coupling constant is proportional to the concentration N of exciton species: $\Omega \propto \sqrt{N}$. [37] According to the predictions of Figure 1b, and the results on Figure 2a, the extent of cancellation of absorption does not reach 0 due to the fact that $\gamma_x^{\mathrm{nr}} \neq 0$. The dashed line in Figure 2c was obtained by extending the coupled–mode theory to account for the interactions of three oscillators (cavity, plasmon and exciton) with light (see supporting information). The spectral bands located at $\omega_\pm$ exhibit the asymmetric near–perfect absorption of light (Figure 1f), which occur due to asymmetry in the radiative rates of the uncoupled excitons and the P_+ state.

The cavity–plasmon–exciton interactions can be visualised in a hybridisation diagram as

shown in Figure 3b. The interaction of the FP (FP, with energy $\hbar\omega_c$) and LSPRs (LSPR, with energy $\hbar\omega_p$, noting that in the most general case $\omega_p \neq \omega_c$) results in the formation of the $P_\pm$ hybrid states, one of which is nearly resonant with the excitons of PIC J–aggregates (exciton energy is $\hbar\omega_x$). Coherent plasmon–exciton–cavity states arise, and due to a modification of the radiative rate of the particle plasmons γ_p^{r}, these coherent states approach a critical coupling condition resulting in near–perfect absorption of light at their corresponding resonance frequencies. Coherent states have been touted to increase the efficiency of photo–induced charge separation processes.[22,38] In the following, we explore the potential for our system to exhibit these effects.

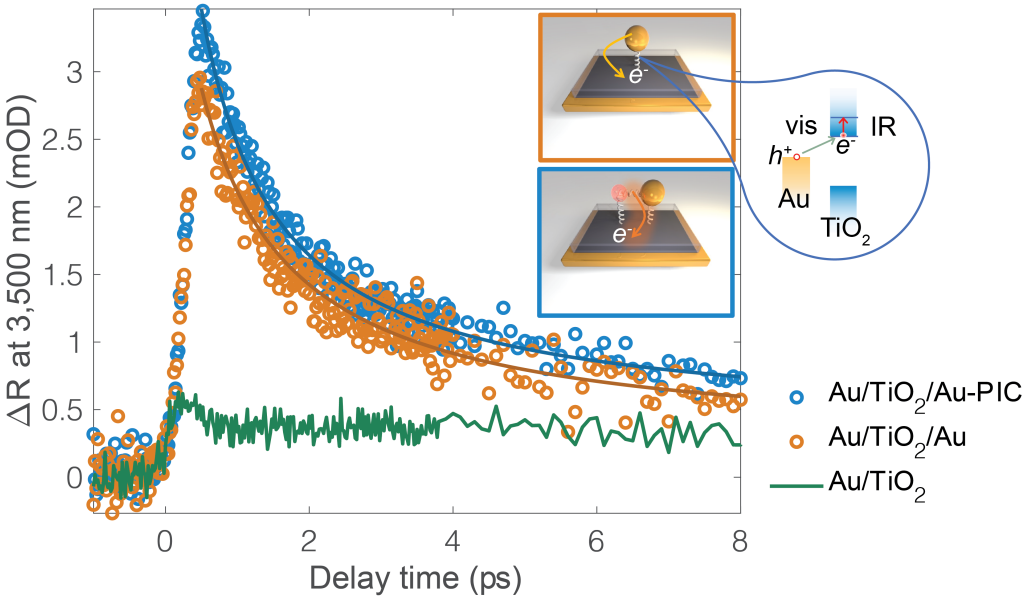

Figure 4: **Photo–induced charge separation**. Photo–excitation with visible light ("vis", green arrow in inset, pump pulses centered at 580 nm) creates a transient population of electrons in the conduction band of TiO_2, which can be probed by measuring changes in the reflectance (ΔR) of time–delayed infrared light pulses ("IR", red arrow, wavelength: 3.5 μm). The plot shows measured ΔR *vs* pump–probe delay times for Au/TiO_2/Au and Au/TiO_2/Au-PIC samples. Also shown for reference is a control Au/TiO_2 film.

Photo–induced electron transfer from metal nanostructures into supporting semiconductor materials is thought to occur following non–radiative (Landau) damping of LSPRs.[39,40] Excitons in J–aggregates of PIC molecules can also be dissociated resulting in charge trans-

fer into an acceptor material,[41] and consequently, the system of Figure 2c has two possible pathways for electron transfer into the TiO_2 support. Distinct charge transfer mechanisms can be evoked when photo–excitation results in a coherent plasmon–exciton superposition state. The branching ratio between charge injection and recombination (not resulting in charge separation) can be controlled by quantum (Fano) interference.[22,38,42]

In order to study charge injection into TiO_2, we excited the samples using ultra–short laser pulses with spectral maxima tuned to the higher–energy hybrid state of the sample (P_+ or ω_+, Figure 3b) and measured changes in the magnitude of reflectance ΔR of 3,500 nm pulses that impinged the sample with a controlled time delay with respect to the arrival of the pump pulses. The pump pulses were lightly focused at normal incidence to the sample surface. The incident pump power was adjusted to be as low as possible (whilst attaining sufficient signal–to–noise) to ensure that the photo–induced processes were linear with the excitation power (see supporting information section Figure S2). Injected electrons in the conduction band of TiO_2 produce reduced TiO_2 species which are known to absorb both visible and infra red light making it possible to detect transient electron populations in the conduction band of TiO_2 by measuring changes in the reflectance of these infrared light pulses.[43–45]

In our system, coherent interactions increase the efficiency of charge separation by a factor of about 1.22 (Figure 4). Immediately after photo–excitation (*i.e.* delay time $\sim$ 0 ps), the amplitude of the ΔR signal for the mirror/TiO_2/Au-PIC structure (blue line, Figure 4) reaches a magnitude of $\sim$ 4.34 mOD which is about 1.22 $\times$ higher than the one obtained for the structure without the exciton material ($\Delta R \sim$ 3.54 mOD, orange line Figure 4). Evidence that the measured transient signals originate from electron transfer into TiO_2 is found in a set of control experiments (supporting information section S4), where we show that transient changes in the reflectivity of the samples only occur in the presence of a Au nanoparticle–TiO_2 interface, in contrast to inert (i.e., no electron accepting states) Au–SiO_2 interfaces, where electron injection from Au nanoparticles is unlikely due to the unfavorable

energetics.[7]

The observed increase in the transient signal is close to the theoretical prediction made by Svidzinsky et al.[22], who predicted that Fano–induced coherence could increase the maximum photo-current from a photo–voltaic device by 1/3. The transient signal measured for the plasmon–exciton system (blue line Figure 4) is larger than the one obtained for the plasmon–cavity system at all pump–probe delay times, further reassuring the difference in transient population of electrons in TiO_2. As a control, Figure 4 also shows the results obtained for a sample consisting of a mirror–semiconductor only, and it indicates that electron injection into the TiO_2 occurs within a sub–picosecond time scale (see supporting information section Figure S1), consistent with previous reports.[44] The decrease in the concentration of electrons in TiO_2 can be accounted for by a second–order kinetic model[46–48] (solid lines in Figure 4, see supporting information section S5 for details) which yields identical decay rates for the mirror/TiO_2/Au and mirror/TiO_2/Au-PIC systems, consistent with electron–hole recombination across the Au nanoparticle–TiO_2 interface, as reported by Bian et al.[44]. Further improvements in photo–induced charge transfer could be achieved by creating the molecular J–aggregates directly on the surface of the metal nanoparticles. This could be achieved through self–assembly approaches,[49] that will place the J–aggregates in areas of intense plasmonic near–field, increasing the plasmon–exciton interaction strength (Ω).

In summary, we have demonstrated a system that simultaneously exhibits coherent plasmon–exciton interactions and high absorption light. The system was described using a coupled–mode theory that fully accounts for the key experimental observations, including the appearance of a classical analogue of electromagnetically induced transparency. We furthermore investigated the effect of the photo–excitation of coherent plasmon–exciton states on photo–induced charge separation, by means of ultra–fast spectroscopy. Our model system opens the prospect for further studies on the effect of strong light–matter coupling on light–driven processes such as electron and energy transfer, which have important implications for photocatalysis and related applications. In this regard, we envisage that structures pos-

sessing higher cavity Q factors, nanoparticles with a narrower size distributions and better structuring of exciton materials (by means of, for instance, self–assembly[49]) could result in augmented coherence which could in turn lead to more drastic and novel effects.

References

(1) Törmä, P.; Barnes, W. L. Strong coupling between surface plasmon polaritons and emitters: a review. *Reports on Progress in Physics* **2015**, *78*, 013901.

(2) Ebbesen, T. W. Hybrid Light–Matter States in a Molecular and Material Science Perspective. *Accounts of Chemical Research* **2016**, *49*, 2403–2412.

(3) Salomon, A.; Genet, C.; Ebbesen, T. Molecule–Light Complex: Dynamics of Hybrid Molecule–Surface Plasmon States. *Angewandte Chemie International Edition* **2009**, *48*, 8748–8751.

(4) Gomez, D.; Lo, S. S.; Davis, T. J.; Hartland, G. V. Pico–Second Kinetics of Strongly Coupled Excitons and Surface Plasmon Polaritons. *The Journal of Physical Chemistry B* **2013**, *117*, 4340–4346.

(5) Hutchison, J. A.; Schwartz, T.; Genet, C.; Devaux, E.; Ebbesen, T. W. Modifying Chemical Landscapes by Coupling to Vacuum Fields. *Angewandte Chemie International Edition* **2012**, *51*, 1592–1596.

(6) Munkhbat, B.; Wersäll, M.; Baranov, D. G.; Antosiewicz, T. J.; Shegai, T. Suppression of photo-oxidation of organic chromophores by strong coupling to plasmonic nanoantennas. *Science Advances* **2018**, *4*, eaas9552.

(7) Zeng, P.; Cadusch, J.; Chakraborty, D.; Smith, T. A.; Roberts, A.; Sader, J.; Davis, T.; Gomez, D. E. Photo-induced electron transfer in the strong coupling regime: Waveguide-plasmon polaritons. *Nano Letters* **2016**, *16*, 2651–2656.

(8) Shan, H. et al. Direct observation of ultrafast plasmonic hot electron transfer in the strong coupling regime. *Light: Science & Applications* **2019**, *8*, 9.

(9) Hutchison, J. A.; Liscio, A.; Schwartz, T.; Canaguier-Durand, A.; Genet, C.; Palermo, V.; Samorì, P.; Ebbesen, T. W. Tuning the Work-Function Via Strong Coupling. *Advanced Materials* **2013**, *25*, 2481–2485.

(10) Orgiu, E.; George, J.; Hutchison, J. A.; Devaux, E.; Dayen, J. F.; Doudin, B.; Stellacci, F.; Genet, C.; Schachenmayer, J.; Genes, C.; Pupillo, G.; Samori, P.; Ebbesen, T. W. Conductivity in organic semiconductors hybridized with the vacuum field. *Nat Mater* **2015**, *14*, 1123–1129.

(11) Yadav, R. K.; Bourgeois, M. R.; Cherqui, C.; Juarez, X. G.; Wang, W.; Odom, T. W.; Schatz, G. C.; Basu, J. K. Room Temperature Weak-to-Strong Coupling and the Emergence of Collective Emission from Quantum Dots Coupled to Plasmonic Arrays. *ACS Nano* **2020**, *14*, 7347–7357.

(12) Aberra Guebrou, S.; Symonds, C.; Homeyer, E.; Plenet, J. C.; Gartstein, Y. N.; Agranovich, V. M.; Bellessa, J. Coherent Emission from a Disordered Organic Semiconductor Induced by Strong Coupling with Surface Plasmons. *Phys. Rev. Lett.* **2012**, *108*, 066401.

(13) Zhong, X.; Chervy, T.; Zhang, L.; Thomas, A.; George, J.; Genet, C.; Hutchison, J. A.; Ebbesen, T. W. Energy Transfer between Spatially Separated Entangled Molecules. *Angewandte Chemie International Edition* **2017**, *56*, 9034–9038.

(14) Zhong, X.; Chervy, T.; Wang, S.; George, J.; Thomas, A.; Hutchison, J. A.; Devaux, E.; Genet, C.; Ebbesen, T. W. Non-Radiative Energy Transfer Mediated by Hybrid Light-Matter States. *Angewandte Chemie International Edition* **2016**, *55*, 6202–6206.

(15) Sun, Y.; Tan, W.; Li, H.-q.; Li, J.; Chen, H. Experimental Demonstration of a Coherent Perfect Absorber with PT Phase Transition. *Phys. Rev. Lett.* **2014**, *112*, 143903.

(16) Zanotto, S.; Mezzapesa, F. P.; Bianco, F.; Biasiol, G.; Baldacci, L.; Vitiello, M. S.; Sorba, L.; Colombelli, R.; Tredicucci, A. Perfect energy-feeding into strongly coupled systems and interferometric control of polariton absorption. *Nat Phys* **2014**, *10*, 830–834.

(17) Higgins, K. D. B.; Benjamin, S. C.; Stace, T. M.; Milburn, G. J.; Lovett, B. W.; Gauger, E. M. Superabsorption of light via quantum engineering. *Nature Communications* **2014**, *5*, 4705.

(18) Peng, P.; Liu, Y.-C.; Xu, D.; Cao, Q.-T.; Lu, G.; Gong, Q.; Xiao, Y.-F. Enhancing Coherent Light-Matter Interactions through Microcavity-Engineered Plasmonic Resonances. *Phys. Rev. Lett.* **2017**, *119*, 233901.

(19) Suh, W.; Wang, Z.; Fan, S. Temporal coupled-mode theory and the presence of non-orthogonal modes in lossless multimode cavities. *IEEE Journal of Quantum Electronics* **2004**, *40*, 1511–1518.

(20) Haus, H. *Waves and fields in optoelectronics*; Prentice-Hall Series in Solid State Physical Electronics; Prentice Hall, 1984.

(21) Fan, S.; Suh, W.; Joannopoulos, J. D. Temporal coupled-mode theory for the Fano resonance in optical resonators. *J. Opt. Soc. Am. A* **2003**, *20*, 569–572.

(22) Svidzinsky, A. A.; Dorfman, K. E.; Scully, M. O. Enhancing photovoltaic power by Fano-induced coherence. *Phys. Rev. A* **2011**, *84*, 053818.

(23) Fleischhauer, M.; Imamoglu, A.; Marangos, J. P. Electromagnetically induced transparency: Optics in coherent media. *Rev. Mod. Phys.* **2005**, *77*, 633–673.

(24) Wang, C.; Jiang, X.; Zhao, G.; Zhang, M.; Hsu, C. W.; Peng, B.; Stone, A. D.; Jiang, L.; Yang, L. Electromagnetically induced transparency at a chiral exceptional point. *Nature Physics* **2020**, *16*, 334–340.

(25) Tassin, P.; Zhang, L.; Zhao, R.; Jain, A.; Koschny, T.; Soukoulis, C. M. Electromagnetically Induced Transparency and Absorption in Metamaterials: The Radiating Two-Oscillator Model and Its Experimental Confirmation. *Phys. Rev. Lett.* **2012**, *109*, 187401.

(26) Papasimakis, N.; Fedotov, V. A.; Zheludev, N. I.; Prosvirnin, S. L. Metamaterial Analog of Electromagnetically Induced Transparency. *Phys. Rev. Lett.* **2008**, *101*, 253903.

(27) Liu, N.; Langguth, L.; Weiss, T.; Kastel, J.; Fleischhauer, M.; Pfau, T.; Giessen, H. Plasmonic analogue of electromagnetically induced transparency at the Drude damping limit. *Nat Mater* **2009**, *8*, 758–762.

(28) DeLacy, B. G.; Miller, O. D.; Hsu, C. W.; Zander, Z.; Lacey, S.; Yagloski, R.; Fountain, A. W.; Valdes, E.; Anquillare, E.; Soljačić, M.; Johnson, S. G.; Joannopoulos, J. D. Coherent Plasmon-Exciton Coupling in Silver Platelet-J-aggregate Nanocomposites. *Nano Letters* **2015**, *15*, 2588–2593, PIC aggregates.

(29) Sweeney, W. R.; Hsu, C. W.; Rotter, S.; Stone, A. D. Perfectly Absorbing Exceptional Points and Chiral Absorbers. *Phys. Rev. Lett.* **2019**, *122*, 093901.

(30) Berkhout, A.; Koenderink, A. F. Perfect Absorption and Phase Singularities in Plasmon Antenna Array Etalons. *ACS Photonics* **2019**, *6*, 2917–2925.

(31) Kwadrin, A.; Osorio, C. I.; Koenderink, A. F. Backaction in metasurface etalons. *Phys. Rev. B* **2016**, *93*, 104301.

(32) Ng, C.; Wesemann, L.; Panchenko, E.; Song, J.; Davis, T. J.; Roberts, A.; Gómez, D. E. Plasmonic Near-Complete Optical Absorption and Its Applications. *Advanced Optical Materials* **2019**, *7*, 1801660.

(33) Shi, X.; Ueno, K.; Oshikiri, T.; Sun, Q.; Sasaki, K.; Misawa, H. Enhanced water splitting under modal strong coupling conditions. *Nature Nanotechnology* **2018**, *13*, 953–958.

(34) Struganova, I. Dynamics of Formation of 1,1'-Diethyl-2,2'-Cyanine Iodide J-Aggregates in Solution. *Journal of Physical Chemistry A* **2000**, *104*, 9670–9674.

(35) Bonin, G. O.; Barrow, S. J.; Connell, T. U.; Roberts, A.; Chesman, A. S. R.; Gomez, D. E. Self-Assembly of Plasmonic Near-Perfect Absorbers of Light: The Effect of Particle Size. *The Journal of Physical Chemistry Letters* **2020**, *11*, 8378–8385.

(36) Ng, C.; Cadusch, J.; Dligatch, S.; Roberts, A.; Davis, T. J.; Mulvaney, P.; Gomez, D. E. Hot Carrier Extraction with Plasmonic Broadband Absorbers. *ACS Nano* **2016**, *10*, 4704–4711.

(37) Thomas, R.; Thomas, A.; Pullanchery, S.; Joseph, L.; Somasundaran, S. M.; Swathi, R. S.; Gray, S. K.; Thomas, K. G. Plexcitons: The Role of Oscillator Strengths and Spectral Widths in Determining Strong Coupling. *ACS Nano* **2018**, *12*, 402–415.

(38) Tomasi, S.; Kassal, I. Classification of Coherent Enhancements of Light-Harvesting Processes. *The Journal of Physical Chemistry Letters* **2020**, *11*, 2348–2355, PMID: 32119554.

(39) Brongersma, M. L.; Halas, N. J.; Nordlander, P. Plasmon-induced hot carrier science and technology. *Nat Nano* **2015**, *10*, 25–34.

(40) Liu, Y.; Chen, Q.; Cullen, D. A.; Xie, Z.; Lian, T. Efficient Hot Electron Transfer from Small Au Nanoparticles. *Nano Letters* **2020**, *20*, 4322–4329.

(41) Kawasaki, M.; Aoyama, S.; Kozawa, E. Enhanced Intra-Aggregate Charge Separation from Binary Excitons in Mixed J-Aggregates of Cyanine Dyes. *The Journal of Physical Chemistry B* **2006**, *110*, 24480–24485.

(42) Schäfer, C.; Ruggenthaler, M.; Appel, H.; Rubio, A. Modification of excitation and charge transfer in cavity quantum-electrodynamical chemistry. *Proceedings of the National Academy of Sciences* **2019**, *116*, 4883–4892.

(43) Tachikawa, T.; Tojo, S.; Fujitsuka, M.; Sekino, T.; Majima, T. Photoinduced Charge Separation in Titania Nanotubes. *The Journal of Physical Chemistry B* **2006**, *110*, 14055–14059.

(44) Bian, Z.; Tachikawa, T.; Zhang, P.; Fujitsuka, M.; Majima, T. Au/TiO2 Superstructure-Based Plasmonic Photocatalysts Exhibiting Efficient Charge Separation and Unprecedented Activity. *Journal of the American Chemical Society* **2014**, *136*, 458–465.

(45) Furube, A.; Du, L.; Hara, K.; Katoh, R.; Tachiya, M. Ultrafast Plasmon-Induced Electron Transfer from Gold Nanodots into TiO_2 Nanoparticles. *Journal of the American Chemical Society* **2007**, *129*, 14852–14853.

(46) Tamaki, Y.; Hara, K.; Katoh, R.; Tachiya, M.; Furube, A. Femtosecond Visible-to-IR Spectroscopy of TiO_2 Nanocrystalline Films: Elucidation of the Electron Mobility before Deep Trapping. *The Journal of Physical Chemistry C* **2009**, *113*, 11741–11746.

(47) Iwata, K.; Takaya, T.; Hamaguchi, H.-o.; Yamakata, A.; Ishibashi, T.-a.; Onishi, H.; Kuroda, H. Carrier Dynamics in TiO_2 and Pt/TiO_2 Powders Observed by Femtosecond Time-Resolved Near-Infrared Spectroscopy at a Spectral Region of 0.9 – 1.5 μm with the Direct Absorption Method. *The Journal of Physical Chemistry B* **2004**, *108*, 20233–20239.

(48) Furube, A.; Asahi, T.; Masuhara, H.; Yamashita, H.; Anpo, M. Charge Carrier Dynamics of Standard TiO_2 Catalysts Revealed by Femtosecond Diffuse Reflectance Spectroscopy. *The Journal of Physical Chemistry B* **1999**, *103*, 3120–3127.

(49) Liu, R.; Zhou, Z.-K.; Yu, Y.-C.; Zhang, T.; Wang, H.; Liu, G.; Wei, Y.; Chen, H.; Wang, X.-H. Strong Light-Matter Interactions in Single Open Plasmonic Nanocavities at the Quantum Optics Limit. *Phys. Rev. Lett.* **2017**, *118*, 237401.

Acknowledgement

We acknowledge the Hokkaido University Overseas Guest Instructor Program, the financial support from JSPS KAKENHI (Grant Nos. JP18H05205, JP18K05053, and JP20K15113), the Nanotechnology Platform (Hokkaido University), the Dynamic Alliance for Open Innovation Bridging Human, Environment and Materials (Five-Star Alliance) of MEXT, the ARC for support through a Future Fellowship (FT140100514) and a Discovery Project (DP160100983).

Competing financial interests The authors declare no competing financial interests

Supporting Information Available

Further details on the coupled mode theory, details on sample preparation and measurements and the effect of PIC concentration on the measured absorption spectrum.

Graphical TOC Entry